Benzodiazepine Analogues. Part 9.[1] Kinetics and Mechanism of the Azidotrimethylsilane-mediated Schmidt Reaction of Flavanones

Perry T. Kaye,* M. Jack Mphahlele and Michael E. Brown
Department of Chemistry, Rhodes University, PO Box 94, Grahamstown, 6140, South Africa

^{1}H NMR spectroscopy has been used to monitor the formation of 1,4-benzoxazepinones and their [1,5-*d*]tetrazolo analogues *via* azidotrimethylsilane-mediated Schmidt rearrangement of flavanone precursors. Analysis of the kinetic data has permitted the determination of rate coefficients and rationalization of substituent effects.

In a previous study,[2] we have shown that Baeyer–Villiger oxidation of flavanones (**1**), with *m*-chloroperbenzoic acid (MCPBA), proceeds regioselectively to afford 1,5-benzodioxepin-2-ones (**2**) (Scheme 1). However, when the same substrates undergo the Schmidt reaction[3] [using azidotrimethylsilane (TMS–N_3) in trifluoroacetic acid] the regioselectivity of heteroatom insertion is completely reversed yielding the 1,4-benzoxazepin-5(4*H*)-ones (**3**) and their [1,5-*d*]tetrazolo derivatives (**4**).[4] To explain these observations, cognate mechanistic studies of both Baeyer–Villiger[5] and Schmidt reactions of flavanones have been undertaken; in this article, we report the results of our research on the latter.

The Schmidt rearrangement of ketones to afford amides is typically achieved using sodium azide in an acidic medium[6] and a number of mechanistic investigations have been reported.[7,8] The generally accepted mechanism involves formation of *syn*- and *anti*-iminodiazonium† ions [*e.g.* intermediate E (Scheme 2)] followed by migration of the *anti*-substituent. For alkyl phenyl ketones, aryl migration appears to be dominant unless the alkyl group is bulky [*e.g.* $(CH_3)_2CH$].[8] The cyclic alkyl phenyl ketones, chroman-4-one and 6-methoxytetralone, however, have been shown by Lockhart *et al.*[9] to afford, *via* alkyl migration, the corresponding 1,4-benzoxazepin-5(4*H*)-one as the sole rearrangement product in each case.‡ Flavanones, on treatment with TMS–N_3 in trifluoroacetic acid, also exhibit exclusive alkyl migration to afford the 2-aryl-1,4-benzoxazepin-5(4*H*)-ones (**3**), but the reaction is complicated by the simultaneous formation of the [1,5-*d*]tetrazolo analogues **4**.[3,4] To our knowledge, no kinetic studies of this reaction system have been reported.

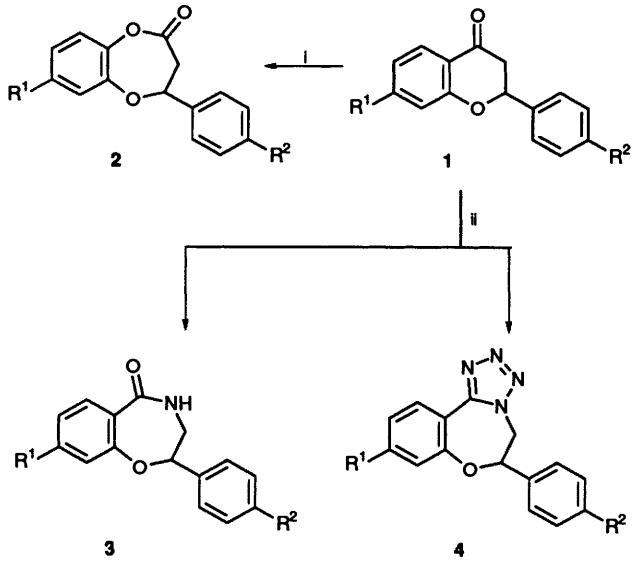

Scheme 1 *Reagents:* (i), MCPBA, CH_2Cl_2; (ii), TMS–N_3, CF_3CO_2H

Experimental

Materials.—The synthesis and characterization of the flavanone precursors, **1**, the 2-aryl-1,4-benzoxazepin-5(4*H*)-ones, (**3a–c, e** and **f** and their [1,5-*d*]tetrazolo derivatives, **4a–c, e** and **f** have been reported elsewhere.[4] Analytical data for new compounds involved in this study are as follows.

8-*Methoxy*-2-*phenyl*-2,3-*dihydro*-1,4-*benzoxazepin*-5(4H)-*one* (**3d**). Mp 164–166 °C (from ethanol) (Found: M^+, 269.1053. $C_{16}H_{15}NO_3$ requires *M*, 269.1052); δ_H(400 MHz; $CDCl_3$) 3.42–3.56 (2 H, m, 3-H), 3.74 (3 H, s, OCH_3), 5.24 (1 H, dd, 2-H), 6.47 (1 H, d, 9-H), 6.57 (1 H, dd, 7-H), 7.33 (5 H, m, ArH) and 7.93 (1 H, d, 6-H); δ_C(100 MHz; $CDCl_3$) 47.7 (C-3), 55.5 (OCH_3), 84.8 (C-2), 105.6, 109.9, 114.6, 126.1, 128.6, 128.7, 134.0, 138.7, 157.5, 164.5 (ArC) and 170.7 (C-5); ν_{max}(KBr)/cm^{-1} 3300 (NH) and 1670 (C=O).

9-*Methoxy*-6-*phenyl*-5,6-*dihydrotetrazolo*[1,5-d]-1,4-*benzoxazepine* (**4d**). Mp 130–132 °C (from ethanol) (Found: C, 65.3; H, 4.9; N, 19.0. $C_{16}H_{14}N_4O_2$ requires C, 65.3; H, 4.8; N, 19.0%); δ_H(400 MHz; $CDCl_3$) 3.83 (3 H, s, OCH_3), 4.80 and 5.08 (2 H, 2 × dd, CH_2), 5.22 (1 H, dd, 6-H), 6.64 (1 H, d, 8-H), 6.81 (1 H, dd, 10-H), 7.41–7.51 (5 H, m, ArH) and 8.46 (1 H, d, 11-H); δ_C(100 MHz; $CDCl_3$) 55.6 (OCH_3), 56.0 (C-5), 79.1 (C-6), 105.4, 105.5, 111.5, 126.1, 129.1, 129.3, 131.6, 136.4, 151.9 and 158.4 (ArC) and 163.6 (C-11b); ν_{max}(KBr)/cm^{-1} 1615 (C=N).

2-(4-*Nitrophenyl*)-2,3-*dihydro*-1,4-*benzoxazepin*-5(4H)-*one* (**3g**). Mp 172–174 °C (from ethanol) (Found: M^+, 284.0797. $C_{15}H_{12}N_2O_4$ requires *M*, 284.0800); δ_H(400 MHz; $CDCl_3$) 3.50 and 3.75 (2 H, 2 × m, CH_2), 5.53 (1 H, t, 2-H), 7.10 (1 H, dd, 9-H), 7.22 (1 H, dd, 7-H), 7.35 (1 H, br, NHCO), 7.50 (1 H, td, 8-H), 7.60 (2 H, d, 2′- and 6′-H), 7.81 (1 H, dd, 6-H) and 8.23 (2 H, d, 3′- and 5′-H); δ_C(100 MHz; $CDCl_3$) 46.0 (C-3), 84.6 (C-2), 122.2, 123.9, 124.4, 126.0, 127.3, 131.0, 133.7, 146.0, 147.9 and 154.0 (ArC) and 170.9 (C-5); ν_{max}(KBr)/cm^{-1} 3500 (NH) and 1660 (C=O).

6-(4-*Nitrophenyl*)-5,6-*dihydrotetrazolo*[1,5-d]-1,4-*benzoxazepine* (**4g**). Mp 198 °C (from ethanol) (Found: M^+, 309.0829. $C_{15}H_{11}N_5O_3$ requires *M*, 309.0862); δ_H(400 MHz; $CDCl_3$) 4.83 and 5.16 (2 H, 2 × dd, CH_2), 5.37 (1 H, d, 6-H), 7.20 (1 H, dd, 8-H), 7.31 (1 H, m, 10-H), 7.50 (1 H, m, 9-H), 7.75 (2 H, d, 2′- and 6′-H), 8.35 (2 H, d, 3′- and 5′-H) and 8.60 (1 H, dd, 11-H); δ_C(100 MHz; $CDCl_3$) 55.9 (C-5), 78.0 (C-6), 112.9, 121.4,

† The orientation of a specified substituent relative to the diazo group.
‡ The possibility of rapid *in situ* hydrolysis of the 1,5-analogues was considered by these authors.

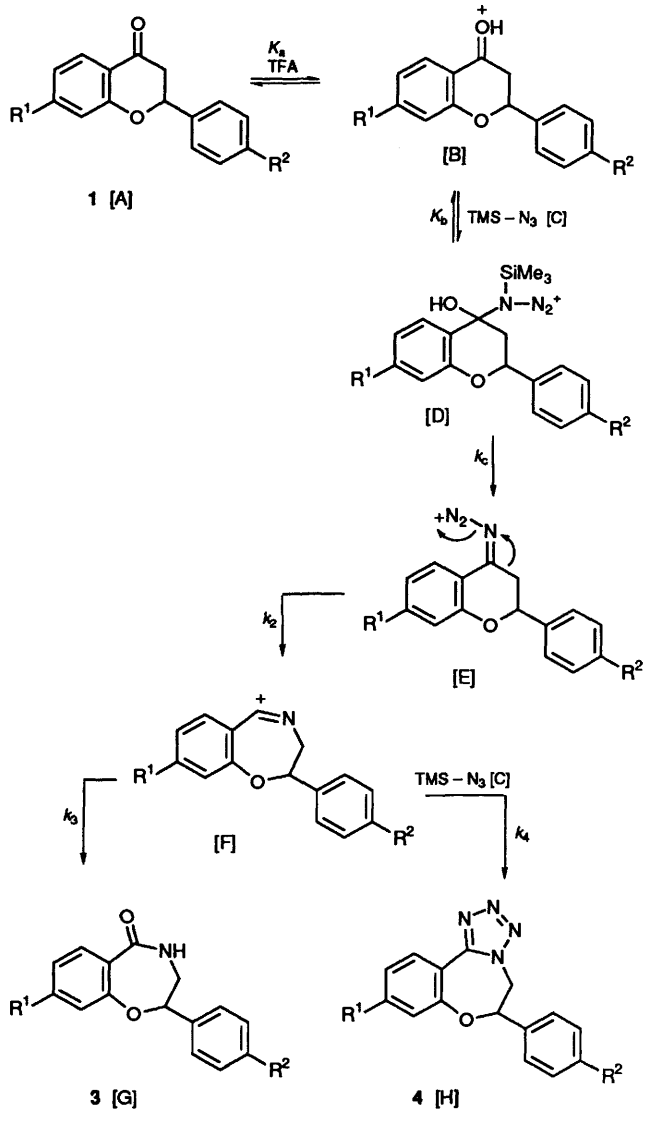

Scheme 2 Mechanistic sequence for the formation of 1,4-benzoxazepines (**3**) and their [1,5-*d*]tetrazolo analogues **4**

124.4, 124.6, 127.1, 130.7, 133.6, 142.9 and 148.6 (ArC) and 156.2 (C-11b); ν_{max}(KBr)/cm^{-1} 1615 (C=N).

Kinetic Procedure.—The reactions were monitored by ^{1}H NMR spectroscopy on a Bruker AMX 400 NMR spectrometer at 303.0 ± 0.1 K. To obviate complications arising from spinning side-bands, the samples were not spun during the kinetic runs.

The flavanone **1** (0.2 mmol) was weighed into an NMR tube, which was immediately sealed with a septum. Trifluoroacetic [^{2}H]acid (TFA) (0.5 cm^3) was then introduced using a syringe and the ^{1}H NMR spectrum of the substrate was obtained. Thereafter, TMS–N_3 (0.042 cm^3, 0.3 mmol) was added by means of a syringe, the mixture was shaken (time, $t = t_0$) and the first spectrum of the reaction mixture was obtained as soon as possible. Subsequent spectra were acquired at 30 min intervals during a reaction period of *ca.* 12 h, corresponding to the consumption of > 50% of the substrate. The total acquisition time for each 32 scan spectrum was 126 s. Concentration changes were determined by integrating the methylene signals for reactants (**1**) and products (**3** and **4**). All kinetic runs were carried out in duplicate and the signals were calibrated relative to the TFA signal at δ 11.3. In each run, the second-order rate coefficient, k_1, was estimated from plots of $(1/[A]_0 - [C]_0) \times \ln([A][C]_0/[C][A]_0)$ *vs.* t [*e.g.* Fig. 1(*a*); see Scheme 3 for notation]. The implicit assumption that the first term in eqn. (2) remains dominant, becomes less justified as the reaction progresses and, not surprisingly, some deviation from linearity was observed in most cases. The value of k_1, thus obtained, was then adjusted to optimise agreement between the experimental and calculated data. Holding k_1 constant and using eqns. (1)–(6), trial values for k_2, k_3 and k_4 were varied until calculated values matched the experimentally determined plots [*e.g.* Figs. 1(*b*) and (*c*)] for the rate of consumption of substrate (A ≡ compound **1**) and the rates of formation of products (G and H, corresponding to compounds **3** and **4**, respectively).

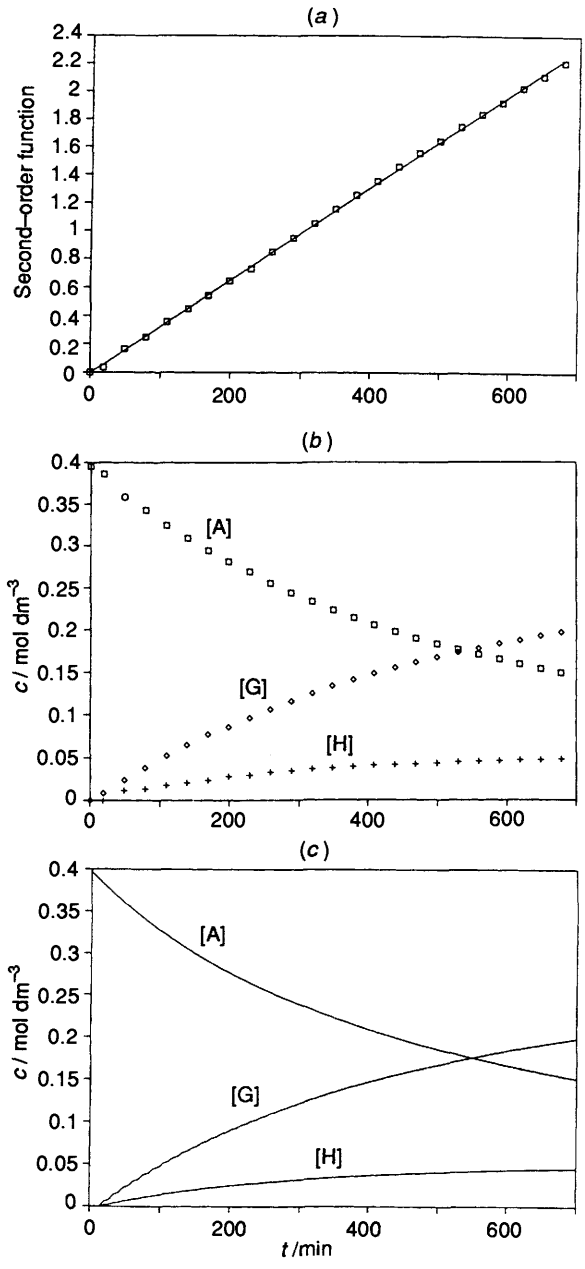

Fig. 1 Kinetic plots for the reaction of compound **1c** with TMS–N_3 in CF_3CO_2D at 303 K, as summarized in Scheme 3. (*a*) Second-order plot for the consumption of substrates A and C. (*b*) Experimental data for the consumption of substrate A and the formation of products G and H. (*c*) Calculated curves, obtained using eqns. (1)–(6).

Results and Discussion

^{1}H NMR spectroscopy proved to be an ideal method for following transformation of the flavonones **1a–g** to the

Table 1 Calculated rate coefficients for the formation of 1,4-benzodiazepines (**3**) and their [1,5-*d*]tetrazolo analogues (**4**) from the corresponding flavanones (**1**)

Substrate			Rate coefficient[a]			
Compd.[b]	R^1	R^2	k_1[c]/dm^3 mol^{-1} min^{-1}	k_2/min^{-1}	k_3/min^{-1}	k_4/dm^3 mol^{-1} min^{-1}
1a	H	H	0.0075	0.20	0.20	0.12
1b	F	H	0.0040	0.28	0.08	0.04
1c	Br	H	0.0033	0.28	0.13	0.06
1d	OCH_3	H	0.0050	0.25	0.06	0.03
1e	H	F	0.0060	0.26	0.14	0.09
1f	H	Br	0.0055	0.28	0.13	0.08
1g	H	NO_2	0.0045	0.25	0.12	0.06

[a] According to Scheme 3. [b] See Scheme 1. [c] Mean of duplicate determinations ($\leqslant \pm 0.0001$ dm^3 mol^{-1} min^{-1}).

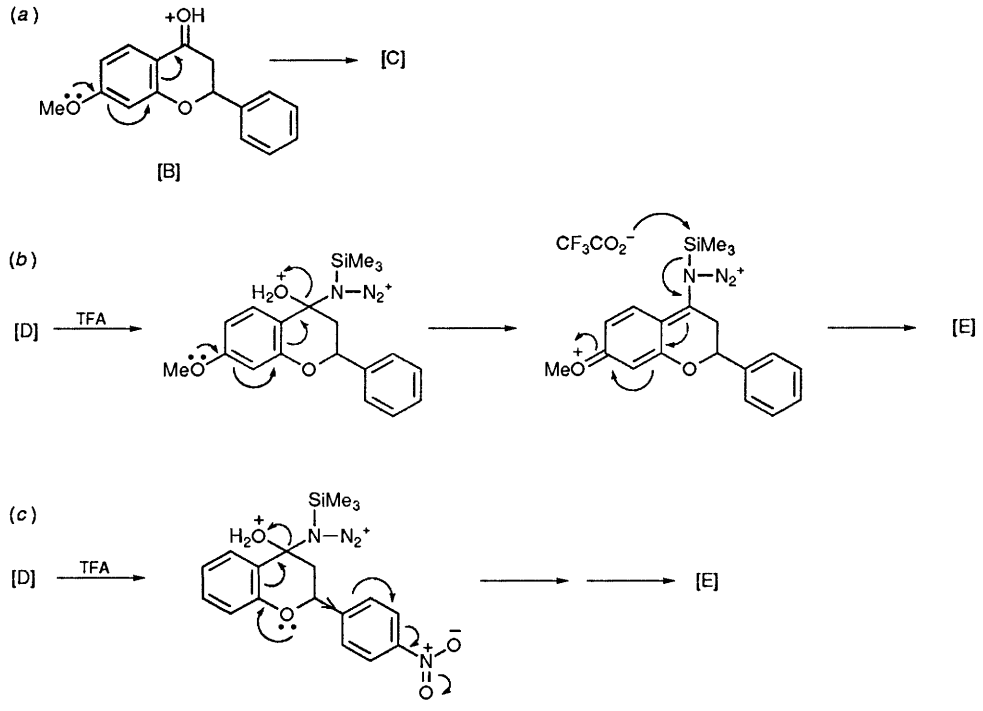

Fig. 2 Substituent effects: (*a*) inhibiting nucleophilic addition; (*b*) enhancing elimination; and (*c*) increasing the −I effect of the 2-aryl group

corresponding 2-aryl-1,4-benzoxazepin-5(4*H*)-ones (**3a–g**) and their [1,5-*d*]tetrazolo derivatives **4a–g**. The spectra clearly indicated the presence of substrate and products, but no accumulation of intermediates was apparent. Analysis of the kinetic data, however, is complicated by (*i*) the simultaneous formation of two different products (**3** and **4**); (*ii*) the involvement of several steps, some of which are assumed to be reversible; and (*iii*) the fact that an additional molecule of TMS–N_3 is consumed in the formation of each molecule of the tetrazolo product **4**. These complications necessitated iterative computer analysis of the data, and for this purpose, the expected mechanism, which is detailed in Scheme 2, was represented by a simplified, consolidated sequence (Scheme 3). Application of the associated eqns. (1)–(6), as described in the Experimental section, afforded values for the rate coefficients (k_1, k_2, k_3 and k_4) for each reaction (Table 1).

The tabulated data revealed several interesting trends.

(*a*) Formation of the iminodiazonium ion intermediate E is rate-limiting in all cases (*i.e.* $k_1 \ll k_2$, k_3 and k_4).

(*b*) The magnitude of the second-order rate coefficient k_1 clearly depends on the nature of the substituent. Formation of intermediate E, however, is expected to involve three steps, two of which are reversible (Scheme 2), and k_1 may therefore be expressed as a composite of the equilibrium constants K_a and K_b

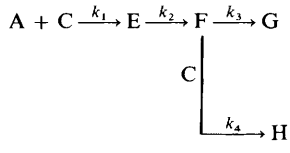

$$-d[A]/dt = k_1[A][C] \quad (1)$$

$$-d[C]/dt = k_1[A][C] + k_4[F][C] \quad (2)$$

$$d[E]/dt = k_1[A][C] - k_2[E] \quad (3)$$

$$d[F]/dt = k_2[E] - k_3[F] - k_4[F][C] \quad (4)$$

$$d[G]/dt = k_3[F] \quad (5)$$

$$d[H]/dt = k_4[F][C] \quad (6)$$

Scheme 3 Consolidated reaction sequence and the associated rate equations used to analyse the kinetic data

and the rate coefficient k_c, *i.e.*, $k_1 = k_c K_a K_b$ (7). Consequently, the observed trends (*e.g.* k_1 for R^1 = H > MeO > F > Br) may be presumed to reflect net substituent effects. Thus, lone

pair delocalization will inhibit the nucleophilic addition step [B ⟶ C; Fig. 2(*a*)] by reducing carbonyl electrophilicity (hence, k_1 for R^1 = H > MeO), but promote the dehydration step§ [D ⟶ E; Fig. 2(*b*)] and hence k_1 for R^1 = MeO > F > Br. In the case of the 4′-substituents R^2, the observed trend (k_1 for R^2 = H > F > Br > NO_2) correlates inversely with overall electron-withdrawing capacity,¶ the −I effect of the 2-aryl substituent inhibiting the dehydration step [D ⟶ E; Fig. 2(*c*)].

(*c*) The actual rearrangement (E ⟶ F) appears to be the fastest step in the process, the overall analysis proving to be relatively insensitive (within certain limits, *viz.*, $0.20 < k_2/\text{min}^{-1} < 0.28$) to variation of the magnitude of k_2. The observed regioselectivity of the rearrangement may be rationalized in terms of lone pair delocalization of the pyran oxygen atom, which (*i*) inhibits aryl migration by increasing the double bond character of the bond between the fused ring and the migration origin [Fig. 3(*a*)][9] and (*ii*) enhances alkyl migration by stabilizing the incipient carbocation [Fig. 3(*b*)]. Thus, for the flavanones **1a–g**, regioselectivity is attributed to transition state factors rather than to the equilibrium populations of the *syn*- and *anti*-iminodiazonium ions E.‖

(*d*) For each substrate, k_3 is approximately twice as large as k_4, an observation which is consistent with the predominant formation of the lactams **3** relative to their [1,5-*d*]tetrazolo derivatives **4**.

Although the rate coefficients k_1 to k_4 obtained for each system do not necessarily constitute unique solution sets, they are, nevertheless, consistent with the mechanism outlined in Scheme 3. Moreover, the analytical approach adopted here

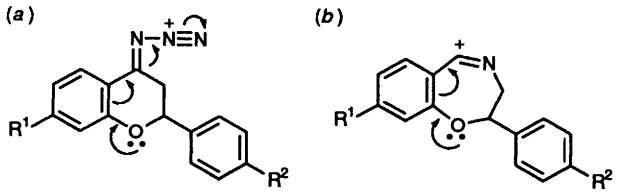

Fig. 3 Involvement of the pyran oxygen in: (*a*) inhibiting aryl migration and (*b*) stabilizing the carbocation generated *via* alkyl migration

provides a useful insight into the complex role of substituents at various stages in this important reaction.

Acknowledgements

The authors thank the *Deutscher Akademischer Austauschdienst* (DAAD) and the Foundation for Research Development (FRD) for bursaries (to M. J. M.) and Rhodes University and the FRD for generous financial support.

References

1 Part 8, P. T. Kaye and M. J. Mphahlele, *Synth. Commun.*, in the press.
2 A. C. Gelebe and P. T. Kaye, *Synth. Commun.*, 1991, **21**, 2263.
3 G. Litkei and T. Patonay, *Acta Chem. Acad. Sci. Hung.*, 1983, **114**, 47.
4 P. T. Kaye and R. D. Whittal, *S. Afr. J. Chem.*, 1991, **44**, 30.
5 The results of this work will be published in due course.
6 See, *e.g.*, D. Huckle, I. M. Lockhart and M. Wright, *J. Chem. Soc.*, 1965, 1137.
7 L. E. Fikes and H. Schechter, *J. Org. Chem.*, 1979, **44**, 741.
8 P. A. S. Smith and J. P. Horwitz, *J. Am. Chem. Soc.*, 1950, **72**, 3718.
9 D. Evans and I. M. Lockhart, *J. Chem. Soc.*, 1965, 4806.
10 N. S. Isaacs, in *Physical Organic Chemistry*, Longman, Harlow, 1987, p. 134.
11 R. Bach and G. J. Wolber, *J. Org. Chem.*, 1982, **47**, 239.

Paper 4/04086D
Received 5*th July* 1994
Accepted 18*th November* 1994

§ Elimination is presumably solvent induced as indicated in Fig. 2(*b*).
¶ See ref. 10 for comparative σ_p^0 values.
‖ A theoretical study of formimino analogues (see ref. 11) has indicated that the magnitude of the nitrogen inversion barriers precludes rapid isomerization between *syn*- and *anti*-iminodiazonium ions. Delocalization effects [*e.g.* Fig. 3(*a*)] may, however, be expected to reduce the inversion barrier significantly.